Skyrmion Crystal from RKKY Interaction Mediated by 2D Electron Gas

Zhentao Wang,[1] Ying Su,[2] Shi-Zeng Lin,[2] and Cristian D. Batista[1,3]
[1]Department of Physics and Astronomy, The University of Tennessee, Knoxville, Tennessee 37996, USA
[2]Theoretical Division, T-4 and CNLS, Los Alamos National Laboratory, Los Alamos, New Mexico 87545, USA
[3]Quantum Condensed Matter Division and Shull-Wollan Center, Oak Ridge National Laboratory, Oak Ridge, Tennessee 37831, USA

(Received 27 November 2019; revised manuscript received 13 February 2020; accepted 5 May 2020; published 19 May 2020)

We consider a C_6 invariant lattice of magnetic moments coupled via a Kondo exchange J with a 2D electron gas (2DEG). The effective Ruderman-Kittel-Kasuya-Yosida interaction between the moments stabilizes a magnetic skyrmion crystal in the presence of magnetic field and easy-axis anisotropy. An attractive aspect of this mechanism is that the magnitude of the magnetic ordering wave vectors, $\boldsymbol{Q}_\nu$ ($\nu = 1, 2, 3$), is dictated by the Fermi wave number k_F: $|\boldsymbol{Q}_\nu| = 2k_F$. Consequently, the topological contribution to the Hall conductivity of the 2DEG becomes of the order of the quantized value, e^2/h, when J is comparable to the Fermi energy ϵ_F.

DOI: 10.1103/PhysRevLett.124.207201

The discovery of magnetic skyrmion crystals (SkX) envisioned by Bogdanov and Yablonskii [1,2] in chiral magnets, such as MnSi, $Fe_{1-x}Co_xSi$, FeGe and Cu_2OSeO_3 [3–7] sparked the interest of the condensed matter community at large and spawned efforts in multiple directions. Among those, identifying the basic ingredients for stabilizing SkX in other materials is one of the most pressing challenges because new stabilization mechanisms are typically accompanied by novel physical properties. For instance, the vector chirality is fixed in the magnetic skyrmions of chiral magnets, such as the so-called B20 compounds; while it is a degree of freedom in the SkX of centrosymmetric materials, such as $BaFe_{1-x-0.05}Sc_xMg_{0.05}O_{19}$, $La_{2-2x}Sr_{1+2x}Mn_2O_7$, Gd_2PdSi_3, and $Gd_3Ru_4Al_{12}$ [8–14]. In the former case, the underlying spiral structure is stabilized by a competition between ferromagnetic exchange and the Dzyaloshinskii-Moriya interaction [15,16]. In contrast, the spiral ordering of centrosymmetric materials arises from competition between different exchange couplings or dipolar interactions [17–21].

To date, most magnetic SkX have been reported in metals, where the interplay between magnetic moments and conduction electrons enables novel response functions, such as the well-known topological Hall effect [22–25] and the current-induced skyrmion motion [26–29]. The topological Hall effect is a direct consequence of the Berry curvature acquired by the reconstructed electronic bands. In the adiabatic limit, the momentum space Berry curvature is controlled by a real space Berry curvature that is proportional to the skyrmion density: each skyrmion produces an effective flux equal to the flux quantum Φ_0. Consequently, Hall conductivities comparable to the quantized value (e^2/h) can in principle be achieved if the ordering wave vector of the SkX is comparable to the Fermi wave vector k_F. As we demonstrate in this Letter, this condition can be naturally fulfilled in f-electron systems where the Ruderman-Kittel-Kasuya-Yosida (RKKY) interaction is mediated by conduction electrons [30–32]. Our results are potentially relevant for the rare earth based materials Gd_2PdSi_3 and $Gd_3Ru_4Al_{12}$ that contain a magnetic field induced SkX phase in their phase diagrams [10–14].

We first demonstrate that the magnetic susceptibility of a 2D electron gas (2DEG) on a C_6 invariant lattice has a maximum at $2k_F$ whenever the single-electron dispersion relation,

$$\epsilon_{\boldsymbol{k}} \approx \frac{1}{2m}(k^2 + uk^4), \tag{1}$$

has a negative quartic correction $u \equiv w/k_F^2 < 0$. Under this condition, a small easy-axis anisotropy is enough to stabilize a magnetic-field induced SkX, which is approximately described by the superposition of three spirals with ordering wave vectors $\boldsymbol{Q}_\nu$ ($\nu = 1, 2, 3$), that are related by $\pm 2\pi/3$ rotations. Given that $|\boldsymbol{Q}_\nu| = 2k_F$, the resulting SkX produce a very large Hall conductivity (of order e^2/h) for a Kondo exchange of $J/\epsilon_F \approx 0.3$. This condition can only be fulfilled in the dilute limit $\epsilon_F \eta(\epsilon_F) \approx (k_F^2 a^2/2\pi) \ll 1$, where $\eta(\epsilon) \approx m/(2\pi)$ is the density of states and a is the lattice constant. Because we are interested in the regime of weak Kondo effect, here we only consider the classical limit of the local magnetic moments.

We start by considering the 2D Kondo lattice model (KLM) for classical magnetic moments:

$$\mathcal{H} = \sum_{\boldsymbol{k}} \sum_{\sigma} (\epsilon_{\boldsymbol{k}} - \mu) c^\dagger_{\boldsymbol{k}\sigma} c_{\boldsymbol{k}\sigma} + J \sum_i \sum_{\alpha\beta} c^\dagger_{i\alpha} \boldsymbol{\sigma}_{\alpha\beta} c_{i\beta} \cdot \boldsymbol{S}_i, \tag{2}$$

where the operator $c^\dagger_{i\sigma}$ ($c_{i\sigma}$) creates (annihilates) an itinerant electron on site i with spin σ, and $c^\dagger_{\boldsymbol{k}\sigma}$ ($c_{\boldsymbol{k}\sigma}$) is

 © 2020 American Physical Society

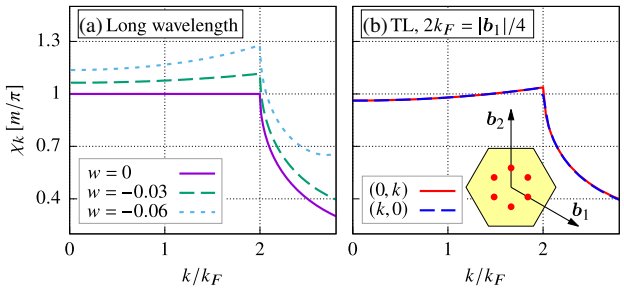

FIG. 1. Susceptibility $\chi_{\boldsymbol{k}}$ for different dispersions. (a) Long wavelength limit Eq. (1), using $V_{\mathrm{BZ}} = (2\pi)^2$; (b) TL Eq. (8) with $2k_F = |\boldsymbol{b}_1|/4$. The inset shows the peak positions of $\chi_{\boldsymbol{k}}$ of the TL in the first BZ, where $\{\boldsymbol{b}_1, \boldsymbol{b}_2\}$ are the reciprocal space basis vectors.

the corresponding Fourier transform. $\epsilon_{\boldsymbol{k}}$ is the bare electron dispersion with chemical potential μ. J is the exchange interaction between the local magnetic moments $\boldsymbol{S}_i$ and the conduction electrons ($\boldsymbol{\sigma}$ is the vector of the Pauli matrices) and $|\boldsymbol{S}_i| = 1$.

In the weak-coupling limit, $J\eta(\epsilon_F) \ll 1$, the interaction between local moments is described by the RKKY model:

$$\mathcal{H}_{\mathrm{RKKY}} = -J^2 \sum_{\boldsymbol{k}} \chi_{\boldsymbol{k}} \boldsymbol{S}_{\boldsymbol{k}} \cdot \boldsymbol{S}_{-\boldsymbol{k}}, \tag{3}$$

with

$$\chi_{\boldsymbol{k}} = -\frac{2}{V_{\mathrm{BZ}}} \int d\boldsymbol{q} \frac{f(\epsilon_{\boldsymbol{q}+\boldsymbol{k}}) - f(\epsilon_{\boldsymbol{q}})}{\epsilon_{\boldsymbol{q}+\boldsymbol{k}} - \epsilon_{\boldsymbol{q}}}, \tag{4}$$

$$\boldsymbol{S}_{\boldsymbol{k}} = \frac{1}{\sqrt{N}} \sum_i e^{i\boldsymbol{k}\cdot\boldsymbol{r}_i} \boldsymbol{S}_i, \tag{5}$$

where N is the number of lattice sites, and $f(\epsilon)$ is the Fermi distribution function.

In general, the RKKY interaction depends on the details of the Fermi surface (FS). However, for small filling fraction, the electronic dispersion relation of C_6 invariant systems can be approximated by Eq. (1) and the FS is circular. In absence of the quartic term ($w = 0$), the susceptibility is flat below $2k_F$ [33] [see Fig. 1(a)],

$$\chi_k = \frac{m}{\pi}\left[1 - \Theta(p-2)\sqrt{1-(2/p)^2}\right], \tag{6}$$

with $p \equiv k/k_F$. The discontinuity of $\partial_k \chi_k$ at $k = 2k_F$ is related to the long-range nature of the RKKY interaction (it decays as $1/r^2$ in real space). The resulting RKKY model is highly frustrated because any spiral ordering with wave number $q \le 2k_F$ is a ground state.

The frustration is partially lifted by a finite quartic term and the magnetic susceptibility becomes

$$\begin{aligned}\chi_k = \frac{m}{\pi|w|p^2\lambda(p,w)}\Bigg[&2\arctan\frac{1}{\lambda(p,w)} \\ &- 2\Theta(p-2)\arctan\frac{\sqrt{1-(2/p)^2}}{\lambda(p,w)} \\ &+ \arctan\frac{|1+wp^2|}{|w|p^2\lambda(p,w)} \\ &- \arctan\frac{\sqrt{(1+wp^2)^2+4w(w+1)}}{|w|p^2\lambda(p,w)}\Bigg],\end{aligned} \tag{7}$$

for $-1 \ll w < 0$ and $p^2 < 2/|w|$, where $\lambda(p,w) \equiv \sqrt{|1+2/(wp^2)|}$. As shown in Fig. 1(a), χ_k is maximized on the ring $k = 2k_F$, where the function χ_k is nonanalytical. As we will see below, the control parameter for the stability of the SkX is the ratio $\chi_{2k_F}/\chi_{k=0}$. According to Eq. (7), $\chi_{2k_F}/\chi_{k=0}$ is determined by $w \equiv uk_F^2$ for $k_F \ll 1$, i.e., w becomes the control parameter in the long wave length regime.

For concreteness, we consider a triangular lattice (TL) with hopping amplitudes $\{t, t_2, t_3\}$ for the first, second, and third nearest neighbors (from now on, we will set $t_2 = t_3 = 0$ unless specified otherwise):

$$\begin{aligned}\epsilon_{\boldsymbol{k}} = &-2t\left[\cos k_x + 2\cos\frac{k_x}{2}\cos\frac{\sqrt{3}k_y}{2}\right] \\ &- 2t_2\left[\cos(\sqrt{3}k_y) + 2\cos\left(\frac{3k_x}{2}\right)\cos\left(\frac{\sqrt{3}k_y}{2}\right)\right] \\ &- 2t_3[\cos(2k_x) + 2\cos k_x \cos(\sqrt{3}k_y)].\end{aligned} \tag{8}$$

The mass m, and w are obtained by expanding $\epsilon_{\boldsymbol{k}}$ near $k = 0$:

$$m = \frac{1}{3(t+3t_2+4t_3)}, \qquad w = -\frac{k_F^2}{16}\frac{t+9t_2+16t_3}{t+3t_2+4t_3}. \tag{9}$$

The resulting magnetic susceptibility, shown in Fig. 1(b), confirms that $\chi_{\boldsymbol{k}}$ is maximized on the $k = 2k_F$ ring. The degeneracy of the ordering wave vectors along the ring direction is lifted by lattice anisotropy terms of order $\mathcal{O}(k^6)$: while the angular dependence of $\chi_{\boldsymbol{k}}$ is very small, a careful numerical integration of Eq. (4) shows only six discrete peaks ($\pm\boldsymbol{Q}_{\nu=1,2,3}$) with the same amplitude [see inset of Fig. 1(b)].

An immediate question is what magnetic structure is stabilized in the presence of magnetic field and easy-axis anisotropy [34]. It has been shown that SkX can arise in hexagonal frustrated Mott insulators whose exchange interactions lead to a similar set of six maxima in the magnetic susceptibility [1,17,18,20]. Indeed, the phase diagram of these materials can be described with a generic Ginzburg-Landau (GL) theory, which only assumes that the

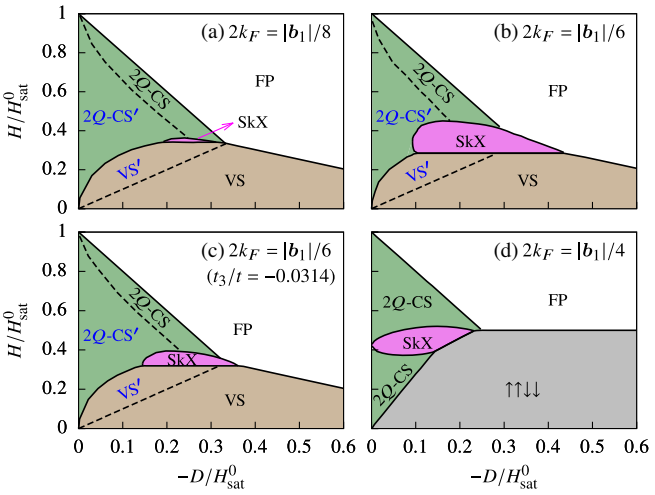

FIG. 2. Phase diagrams of the TL RKKY model with easy-axis single-ion anisotropy in a magnetic field. We set $t_2 = t_3 = 0$ except in (c). (a) $2k_F = |\boldsymbol{b}_1|/8$, which gives $\chi_{2k_F}/\chi_{k=0} \approx 1.0177$, $w \approx -0.013$, $H^0_{\rm sat} \approx 0.0034J^2/t$; (b) $2k_F = |\boldsymbol{b}_1|/6$, which gives $\chi_{2k_F}/\chi_{k=0} \approx 1.0323$, $w \approx -0.023$, $H^0_{\rm sat} \approx 0.0062J^2/t$; (c) $2k_F = |\boldsymbol{b}_1|/6$, which gives $\chi_{2k_F}/\chi_{k=0} \approx 1.0211$, $w \approx -0.013$, $H^0_{\rm sat} \approx 0.0046J^2/t$; (d) $2k_F = |\boldsymbol{b}_1|/4$, which gives $\chi_{2k_F}/\chi_{k=0} \approx 1.0783$, $w \approx -0.051$, $H^0_{\rm sat} \approx 0.016J^2/t$.

magnetic susceptibility is maximized over a ring of wave vectors of the same magnitude and that it is an analytic function of k [19]. The nonanalytical behavior of χ_k at $k = 2k_F$ violates the second assumption, and raises the question of whether the SkX phase can still be stabilized in RKKY systems. Motivated by this question, we add the corresponding Zeeman and anisotropy terms to the TL RKKY Hamiltonian:

$$\mathcal{H}_{\rm total} = \mathcal{H}_{\rm RKKY} + \mathcal{H}', \quad \mathcal{H}' = -H\sum_i S^z_i + D\sum_i (S^z_i)^2. \quad (10)$$

Our Monte Carlo simulation with Metropolis update on finite lattices indeed suggests that the ordering wave number coincides with $2k_F$ at low temperature. However, due to the highly frustrated nature of the RKKY model, the Metropolis update is not efficient enough to overcome freezing into metastable states. We then adopt a $T = 0$ variational approach, which further confirms that the magnetic ordering wave vector has magnitude $Q = 2k_F$ [35].

Figure 2 shows the $T = 0$ phase diagrams for $2k_F = \{|\boldsymbol{b}_1|/8, |\boldsymbol{b}_1|/6, |\boldsymbol{b}_1|/4\}$ including seven different phases, namely, the vertical spiral (VS), vertical spiral with in-plane modulation (VS′), $2\boldsymbol{Q}$-conical spiral ($2\boldsymbol{Q}$-CS), $2\boldsymbol{Q}$-conical spiral with unequal in-plane structure factor intensities ($2\boldsymbol{Q}$-CS′), up-up-down-down (↑↑↓↓), SkX, and the fully polarized (FP) phases (see Fig. 3).

The phase diagrams shown in Fig. 2 are similar to the one obtained from short-range Heisenberg models on the TL [18], and more generally, from a GL analysis of

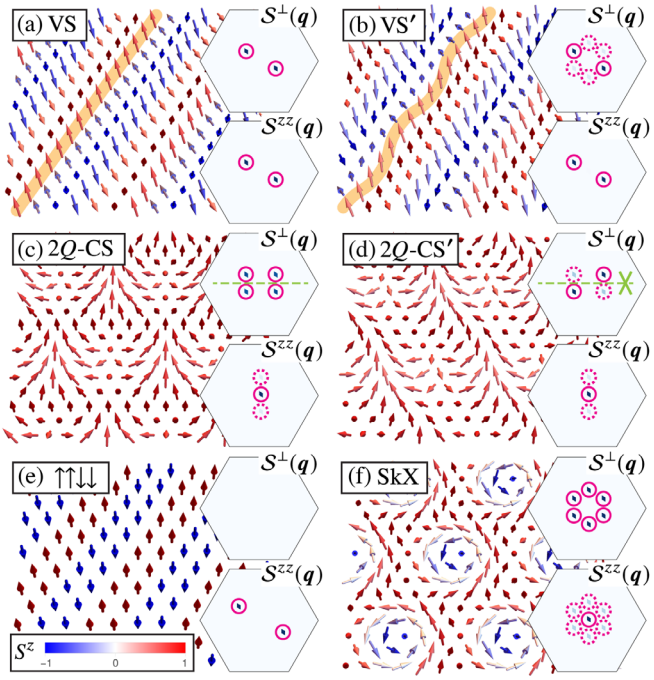

FIG. 3. Spin configurations of phases shown in Fig. 2. The insets show the in-plane ($\mathcal{S}^{\perp}$) and out-of-plane ($\mathcal{S}^{zz}$) static structure factors in the first BZ. The solid (dotted) circles highlight the dominant (subdominant) peaks. The orange markups in (a),(b) highlight the difference between VS and VS′, i.e., absence or presence of the in-plane modulation. The green markups in insets of (c),(d) show the difference between $2\boldsymbol{Q}$-CS and $2\boldsymbol{Q}$-CS′: the former is invariant under a mirror reflection of the xz plane followed by a π rotation along the x axis, while the latter does not respect this symmetry.

the inversion-symmetric magnets [19]. However, there is an important qualitative difference associated with the stability of the SkX phase.

A direct comparison between Figs. 2(a) and 2(b) suggests that the size of the SkX phase depends sensitively on the ratio $\chi_{2k_F}/\chi_{k=0}$, which is controlled by the parameter w from the long wavelength analysis [see Eq. (7)]. To reveal the role of w, we keep $2k_F = |\boldsymbol{b}_1|/6$ and add a finite t_3, that changes w from -0.023 to -0.013 [see Fig. 2(c)]. The SkX phase shrinks as we decrease $|w|$ while keeping $2k_F$ unchanged [Figs. 2(b) and 2(c)]. Indeed, our variational approach confirms that the SkX phase disappears for $|w| \lesssim 0.0115$ when using χ_k given by Eq. (7) (valid for $k_F \ll 1$). In other words, the SkX phase is stable in the *mesoscale* regime $k_F > \sqrt{0.0115/|u|}$.

This behavior is qualitatively different from the GL theory, where the phase diagram, including the SkX phase, remains invariant upon approaching the Lifshitz transition [19]. The key difference is in the relative difference between $(\chi_{2k_F} - \chi_{k=0})$ that determines the saturation field $H^0_{\rm sat} \equiv 2J^2(\chi_{2k_F} - \chi_{k=0})$, and $(\chi_{2k_F} - \chi_{k_n})$ for $\boldsymbol{k}_n = \sum_{\nu=1,3} n_\nu \boldsymbol{Q}_\nu$ (n_ν are *small* integer numbers and $|\boldsymbol{k}_n| > Q$) that determines the exchange energy of the higher

harmonics present in most of the phases, including the SkX. In the GL theory, both energy scales remain comparable for $Q \to 0$. In contrast, $(\chi_{2k_F} - \chi_{k_n})$ becomes much bigger than $(\chi_{2k_F} - \chi_{k=0})$ for $k_F \to 0$ because the slope of χ_k diverges for $k \to 2k_F^+$. This difference becomes less important for $\sqrt{0.0115/|u|} < k_F < 1$, explaining why the phase diagrams of both theories become very similar in the mesoscale regime.

Figures 2(a) and 2(c) show the phase diagrams obtained for the same value of w and different values of $2k_F$ ($2k_F = |\boldsymbol{b}_1|/6$ and $2k_F = |\boldsymbol{b}_1|/8$). The difference between both phase diagrams is produced by small deviations of χ_k from the universal expression in Eq. (7). The size of the SkX phase is bigger for $2k_F = |\boldsymbol{b}_1|/6$ simply because $\chi_{2k_F}/\chi_{k=0}$ is bigger.

For large enough $2k_F$, the long wavelength analysis is no longer accurate and the phase diagram can become qualitatively different from the one obtained for small ordering wave numbers. This is illustrated by Fig. 2(d) for $2k_F = |\boldsymbol{b}_1|/4$: the low field VS and VS′ phases are replaced with a collinear $\uparrow\uparrow\downarrow\downarrow$ ordering, and the low field $2\boldsymbol{Q}$-CS′ phase is replaced by the $2\boldsymbol{Q}$-CS phase. Interestingly, we find that the SkX phase remains robust.

The SkX phase induces nontrivial Berry curvature and anomalous Hall response when coupled to itinerant electrons [22–25]. Figures 4(a) and 4(b) show the folded unreconstructed electronic band structure ($J = 0$) and the FS in the reduced BZ ($2k_F = |\boldsymbol{b}_1|/6$). A finite coupling J opens a gap at the M and K points [Fig. 4(c)]. The lowest two bands develop nonzero Berry curvature $\Omega_n(\boldsymbol{k})$ centered at K and K', where the electron wave functions have the largest renormalization [Figs. 4(d) and 4(e)]. We note that the two lowest bands have the same Chern number: both $C_n = 1$ or $C_n = -1$, where the sign is determined by the sign of the scalar spin chirality.

Figure 4(f) shows the transverse conductivity σ_{xy} [40] of the TL KLM in the SkX phase with fixed electron fillings. A large σ_{xy} can be achieved even in the weak-coupling regime ($J/t \ll 1$), and its magnitude increases quickly upon approaching the long wavelength limit. Such a behavior is *opposite* to the conventional understanding based on the strong-coupling or adiabatic limit. The skyrmion density is no longer dictated by k_F in that limit and it is typically much smaller than the electron density. Thus, a larger skyrmion density (bigger Q) produces larger effective magnetic field and consequently a larger Hall response in the strong-coupling limit.

The k_F-dependence of σ_{xy} can be understood in a simple way. In Fig. 4(b), we see that the FS already occupies 91% of the folded first BZ. σ_{xy} becomes large (of order e^2/h) when the states near K and K' points (where most of the Berry curvature concentrates) are pushed below the Fermi level. This condition is fulfilled when the gap, of order J, becomes comparable to the energy difference between ϵ_K and ϵ_{k_F}:

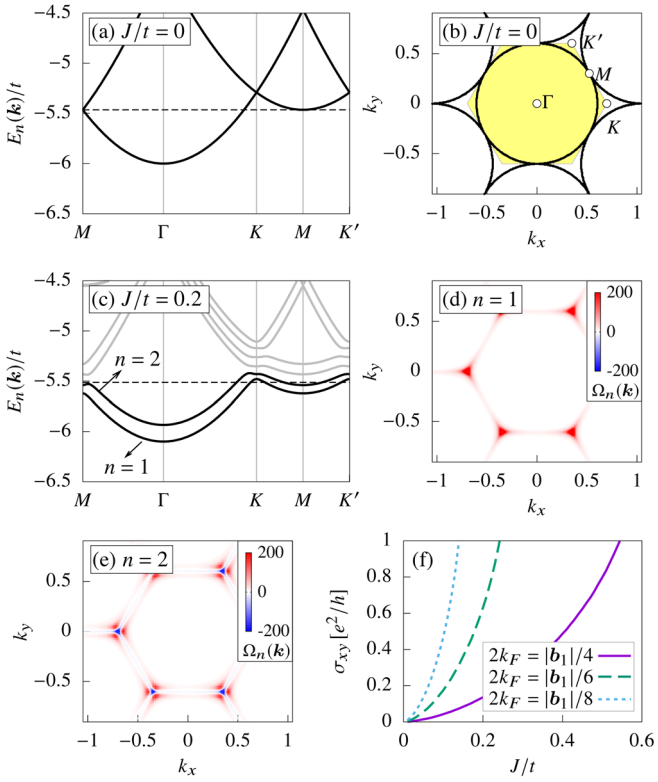

FIG. 4. (a),(b) Electronic band structure and FS of the TL KLM in the folded first BZ ($2k_F = |\boldsymbol{b}_1|/6$) with $J = 0$. (c)–(e) Electronic band structure and Berry curvatures of the lowest two bands in the folded first BZ ($2k_F = |\boldsymbol{b}_1|/6$) with $J/t = 0.2$ and SkX spin configuration. (f) Transverse conductivities of the TL KLM with SkX spin configurations of different Q, at fixed electron filling fractions. The horizontal dashed lines in (a),(c) show the Fermi level for fixed filling $n_c \approx 0.0252$. We use SkX spin configuration obtained at $\{D = -0.002J^2/t, H = 0.007J^2/t\}$ for $2k_F = |\boldsymbol{b}_1|/4$, $\{D = -0.0015J^2/t, H = 0.002J^2/t\}$ for $2k_F = |\boldsymbol{b}_1|/6$, and $\{D = -0.0008J^2/t, H = 0.00117J^2/t\}$ for $2k_F = |\boldsymbol{b}_1|/8$.

$$J \sim \frac{k_F}{m}\left(\frac{2}{\sqrt{3}}k_F - k_F\right) \approx 0.155\frac{k_F^2}{m} \approx 0.3\epsilon_F. \quad (11)$$

In other words, in agreement with the result shown in Fig. 4(f), the value of J required to produce a large anomalous Hall effect is smaller for smaller values of k_F. In fact, the three curves shown in Fig. 4(f) collapse into a single curve after rescaling the x axis to $J/(tk_F^2)$.

To summarize, we find that the quartic term in the dispersion of a 2DEG induces susceptibility maxima at $Q = 2k_F$, which is key to produce a finite saturation field and to stabilize the spiral ordering that is the basis for generating SkX via RKKY interactions. The $T = 0$ phase diagram includes a sizable SkX phase induced by easy-axis anisotropy and a magnetic field. The size of the SkX phase and its stability range is controlled by $\chi_{2k_F}/\chi_{k=0}$, which is in turn determined by w for $k_F \ll 1$. The same electrons

which induce the RKKY interaction and the SkX phase, exhibit a large anomalous Hall *counter-response*, whose magnitude depends solely on $J/(tk_F^2)$ in the weak-coupling limit. This strong feedback effect distinguishes the stabilization mechanism based on the RKKY interaction from other mechanisms in which the lattice parameter of the SkX and the Fermi wave-length are independent length scales.

We note that the $\mathcal{O}(k^4)$ correction in the quasi-particle dispersion relation (1) is not the only way of lifting the spin susceptibility degeneracy of the 2DEG for $k < 2k_F$. For example, the electron-electron interactions can also induce a global maximum of χ_k at a finite wave number close to $2k_F$ [41–51]. Additional magnetic interactions, such as short-range superexchange and dipolar coupling can produce a similar effect. It is also important to note, that four-spin and higher order interactions, not included in the RKKY Hamiltonian, are naturally generated from the KLM upon moving away from the weak-coupling limit [21,52–58]. These higher order terms can also stabilize multi-$\boldsymbol{Q}$ magnetic orderings that include SkX phases [21,54–58]. A variational treatment like the one that has been presented in this Letter can be applied to the full KLM to determine if the effective higher order spin interactions can further stabilize the field-induced SkX phase.

Our results are potentially relevant for explaining the giant topological Hall response of Gd_2PdSi_3 [10,11], which is produced by a field induced SkX phase, as it has been recently revealed by resonant x-ray scattering [12,59]. Indeed, angle-resolved photoemission spectroscopy suggests that RKKY is the dominant interaction in this material [60]. More generally, SkX phases induced by RKKY interactions are expected to be realized in a wider range of hexagonal intermetallic compounds with in-plane spiral ordering (ordering wave vector parallel to the plane) and moderate easy-axis anisotropy.

We thank K. Barros and H. Ishizuka for helpful discussions. Z. W. and C. D. B. are supported by funding from the Lincoln Chair of Excellence in Physics. The work at Los Alamos National Laboratory (LANL) was carried out under the auspices of the U.S. DOE NNSA under Contract No. 89233218CNA000001 through the LDRD Program, and was supported by the Center for Nonlinear Studies at LANL. This research used resources of the Oak Ridge Leadership Computing Facility at the Oak Ridge National Laboratory, which is supported by the Office of Science of the U.S. Department of Energy under Contract No. DE-AC05-00OR22725.

[1] A. N. Bogdanov and D. A. Yablonskii, Zh. Eksp. Teor. Fiz. **95**, 178 (1989) [Sov. Phys. JETP **68**, 101 (1989)].
[2] U. K. Rößler, A. N. Bogdanov, and C. Pfleiderer, Nature (London) **442**, 797 (2006).
[3] S. Mühlbauer, B. Binz, F. Jonietz, C. Pfleiderer, A. Rosch, A. Neubauer, R. Georgii, and P. Böni, Science **323**, 915 (2009).
[4] X. Z. Yu, Y. Onose, N. Kanazawa, J. H. Park, J. H. Han, Y. Matsui, N. Nagaosa, and Y. Tokura, Nature (London) **465**, 901 (2010).
[5] X. Z. Yu, N. Kanazawa, Y. Onose, K. Kimoto, W. Z. Zhang, S. Ishiwata, Y. Matsui, and Y. Tokura, Nat. Mater. **10**, 106 (2011).
[6] S. Seki, X. Z. Yu, S. Ishiwata, and Y. Tokura, Science **336**, 198 (2012).
[7] T. Adams, A. Chacon, M. Wagner, A. Bauer, G. Brandl, B. Pedersen, H. Berger, P. Lemmens, and C. Pfleiderer, Phys. Rev. Lett. **108**, 237204 (2012).
[8] X. Yu, M. Mostovoy, Y. Tokunaga, W. Zhang, K. Kimoto, Y. Matsui, Y. Kaneko, N. Nagaosa, and Y. Tokura, Proc. Natl. Acad. Sci. U.S.A. **109**, 8856 (2012).
[9] X. Z. Yu, Y. Tokunaga, Y. Kaneko, W. Z. Zhang, K. Kimoto, Y. Matsui, Y. Taguchi, and Y. Tokura, Nat. Commun. **5**, 3198 (2014).
[10] R. Mallik, E. V. Sampathkumaran, P. L. Paulose, H. Sugawara, and H. Sato, Pramana—J. Phys. **51**, 505 (1998).
[11] S. R. Saha, H. Sugawara, T. D. Matsuda, H. Sato, R. Mallik, and E. V. Sampathkumaran, Phys. Rev. B **60**, 12162 (1999).
[12] T. Kurumaji, T. Nakajima, M. Hirschberger, A. Kikkawa, Y. Yamasaki, H. Sagayama, H. Nakao, Y. Taguchi, T.-h. Arima, and Y. Tokura, Science **365**, 914 (2019).
[13] V. Chandragiri, K. K. Iyer, and E. V. Sampathkumaran, J. Phys. Condens. Matter **28**, 286002 (2016).
[14] M. Hirschberger, T. Nakajima, S. Gao, L. Peng, A. Kikkawa, T. Kurumaji, M. Kriener, Y. Yamasaki, H. Sagayama, H. Nakao, K. Ohishi, K. Kakurai, Y. Taguchi, X. Yu, T.-h. Arima, and Y. Tokura, Nat. Commun. **10**, 5831 (2019) .
[15] I. Dzyaloshinsky, J. Phys. Chem. Solids **4**, 241 (1958).
[16] T. Moriya, Phys. Rev. **120**, 91 (1960).
[17] T. Okubo, S. Chung, and H. Kawamura, Phys. Rev. Lett. **108**, 017206 (2012).
[18] A. O. Leonov and M. Mostovoy, Nat. Commun. **6**, 8275 (2015).
[19] S.-Z. Lin and S. Hayami, Phys. Rev. B **93**, 064430 (2016).
[20] S. Hayami, S.-Z. Lin, and C. D. Batista, Phys. Rev. B **93**, 184413 (2016).
[21] C. D. Batista, S.-Z. Lin, S. Hayami, and Y. Kamiya, Rep. Prog. Phys. **79**, 084504 (2016).
[22] M. Onoda, G. Tatara, and N. Nagaosa, J. Phys. Soc. Jpn. **73**, 2624 (2004).
[23] S. D. Yi, S. Onoda, N. Nagaosa, and J. H. Han, Phys. Rev. B **80**, 054416 (2009).
[24] K. Hamamoto, M. Ezawa, and N. Nagaosa, Phys. Rev. B **92**, 115417 (2015).
[25] B. Göbel, A. Mook, J. Henk, and I. Mertig, Phys. Rev. B **95**, 094413 (2017).
[26] F. Jonietz, S. Mühlbauer, C. Pfleiderer, A. Neubauer, W. Münzer, A. Bauer, T. Adams, R. Georgii, P. Böni, R. A. Duine, K. Everschor, M. Garst, and A. Rosch, Science **330**, 1648 (2010).
[27] X. Z. Yu, N. Kanazawa, W. Z. Zhang, T. Nagai, T. Hara, K. Kimoto, Y. Matsui, Y. Onose, and Y. Tokura, Nat. Commun. **3**, 988 (2012).

[28] T. Schulz, R. Ritz, A. Bauer, M. Halder, M. Wagner, C. Franz, C. Pfleiderer, K. Everschor, M. Garst, and A. Rosch, Nat. Phys. **8**, 301 (2012).
[29] N. Nagaosa and Y. Tokura, Nat. Nanotechnol. **8**, 899 (2013).
[30] M. A. Ruderman and C. Kittel, Phys. Rev. **96**, 99 (1954).
[31] T. Kasuya, Prog. Theor. Phys. **16**, 45 (1956).
[32] K. Yosida, Phys. Rev. **106**, 893 (1957).
[33] G. F. Giuliani and G. Vignale, *Quantum Theory of the Electron Liquid* (Cambridge University Press, Cambridge, England, 2008).
[34] The easy-axis anisotropy is generated by the combined effect of the spin-orbit coupling and the crystal field on the magnetic ion.
[35] See the Supplemental Material at http://link.aps.org/supplemental/10.1103/PhysRevLett.124.207201 for the description of the variational method and formulae of the Berry related quantities, which include Refs. [36–39].
[36] S. G. Johnson, The NLopt nonlinear-optimization package, http://github.com/stevengj/nlopt.
[37] T. Rowan, Ph.D. thesis, Department of Computer Sciences, University of Texas at Austin, 1990.
[38] A. Bogdanov and A. Hubert, J. Magn. Magn. Mater. **138**, 255 (1994).
[39] D. Vanderbilt, *Berry Phases in Electronic Structure Theory* (Cambridge University Press, Cambridge, England, 2018).
[40] D. Xiao, M.-C. Chang, and Q. Niu, Rev. Mod. Phys. **82**, 1959 (2010).
[41] D. Belitz, T. R. Kirkpatrick, and T. Vojta, Phys. Rev. B **55**, 9452 (1997).
[42] D. S. Hirashima and H. Takahashi, J. Phys. Soc. Jpn. **67**, 3816 (1998).
[43] A. V. Chubukov and D. L. Maslov, Phys. Rev. B **68**, 155113 (2003).
[44] S. Gangadharaiah, D. L. Maslov, A. V. Chubukov, and L. I. Glazman, Phys. Rev. Lett. **94**, 156407 (2005).
[45] A. V. Chubukov, D. L. Maslov, S. Gangadharaiah, and L. I. Glazman, Phys. Rev. B **71**, 205112 (2005).
[46] D. L. Maslov, A. V. Chubukov, and R. Saha, Phys. Rev. B **74**, 220402(R) (2006).
[47] G. Schwiete and K. B. Efetov, Phys. Rev. B **74**, 165108 (2006).
[48] I. L. Aleiner and K. B. Efetov, Phys. Rev. B **74**, 075102 (2006).
[49] A. Shekhter and A. M. Finkel'stein, Phys. Rev. B **74**, 205122 (2006).
[50] P. Simon, B. Braunecker, and D. Loss, Phys. Rev. B **77**, 045108 (2008).
[51] O. Prus, Y. Yaish, M. Reznikov, U. Sivan, and V. Pudalov, Phys. Rev. B **67**, 205407 (2003).
[52] S. Kumar and J. van den Brink, Phys. Rev. Lett. **105**, 216405 (2010).
[53] Y. Akagi, M. Udagawa, and Y. Motome, Phys. Rev. Lett. **108**, 096401 (2012).
[54] D. Solenov, D. Mozyrsky, and I. Martin, Phys. Rev. Lett. **108**, 096403 (2012).
[55] S. Hayami and Y. Motome, Phys. Rev. B **90**, 060402(R) (2014).
[56] R. Ozawa, S. Hayami, K. Barros, G.-W. Chern, Y. Motome, and C. D. Batista, J. Phys. Soc. Jpn. **85**, 103703 (2016).
[57] R. Ozawa, S. Hayami, and Y. Motome, Phys. Rev. Lett. **118**, 147205 (2017).
[58] S. Hayami, R. Ozawa, and Y. Motome, Phys. Rev. B **95**, 224424 (2017).
[59] M. D. Frontzek, Ph.D. thesis, Technische Universität Dresden, 2009.
[60] D. S. Inosov, D. V. Evtushinsky, A. Koitzsch, V. B. Zabolotnyy, S. V. Borisenko, A. A. Kordyuk, M. Frontzek, M. Loewenhaupt, W. Löser, I. Mazilu, H. Bitterlich, G. Behr, J.-U. Hoffmann, R. Follath, and B. Büchner, Phys. Rev. Lett. **102**, 046401 (2009).